A Two-loop Performance Oriented Tip Tracking Control of A Linear Motor Driven Flexible Beam System with Experiments

Lu Lu, *Student Member, IEEE*, Zheng Chen *Student Member, IEEE*, Bin Yao, *Senior Member, IEEE*, and Qingfeng Wang, *Member, IEEE*

***Abstract*—In this paper, a two-loop control structure for the constrained tip regulation of a linear motor driven flexible beam is developed to achieve high performance. Specifically, in the inner loop, a feedback control law with freely assignable closed-loop poles is designed to achieve arbitrarily good disturbance rejection capability at steady state. In the outer loop, an online trajectory replanning unit is constructed so that the tip position output of the beam converges to its desired target as fast as possible while all the constraints of the system are satisfied. Theoretically, it is shown that the proposed approach can achieve sufficiently fast transient converging speed of the tracking error and a guaranteed steady-state tracking accuracy. The proposed strategy is tested on a HIWIN linear motor driven stage system with a flexible beam clamped. Experimental results obtained demonstrate the effectiveness and applicability of the proposed approach.**

***Index Terms*—Flexible structures, Trajectory planning, Constrained Control, Input saturation.**

I. Introduction

Robot manipulators are widely used in different scientific researches and industrial applications [1], [2], [3], [4]. Traditionally, the robot manipulators are built with high stiffness so that they can be treated rigidly and controlled easily. However, the larger size of the actuators, the limitation of the maximum acceleration of the system, and the higher energy consumptions during the control process are also of significant problems [5]. Alternatively, more and more lightweight robot manipulators are designed and used in real applications to achieve faster motion and smaller energy consumption. However, flexibility of the lightweight robot cannot be ignored anymore when doing high speed motion control. It is known that, in order to have good steady-state tracking accuracy, higher feedback gains have to be used to suppress disturbances of the system, which will inevitably excite the lower flexible modes of the lightweight manipulator and make the closed-loop system unstable when these modes are neglected in the controller design stage.

Various types of control techniques have been designed and applied to improve the performance of flexible-link robot systems, which can be classified into two categories: non-model based approach [6], [7] and model-based methods [8], [9], [10], [11], [12], [13]. In non-model based boundary controls [6], [7], simple PD-type feedback control laws with collocated local feedback and actuation are used to dissipate the total energy of the system for stability. Though easier to implement due to simplicity of these energy-based control laws, transient responses of the resulting closed-loop system tend to be poor as there is no direct link between the tunable controller parameters and the closed-loop performance. On the other hand, model-based approaches are mainly based on the truncated finite-dimensional models of the system. Specifically, the linear quadratic (LQ) control with an observer is used in [8] to synthesize a feedback control law to dampen the vibration caused by flexible modes when tracking the reference hub angle. Singular perturbation theory is applied in [9] to decompose the flexible-link manipulator into slow and fast subsystems and a composite controller is designed. Trajectory tracking control of a one-link flexible arm using feedback linearization is discussed in [10], in which the issue of output tracking control with non-minimum phase zeros becomes clear. A two-part linear feedback controller is developed in [11] to deal with the end-point tracking problem with non-minimum phase, in which the model uncertainties such as the Coulomb friction at the joint are not properly addressed and the closed-loop systems has the integrator windup problem for large movements. To deal with model uncertainties due to parameter variations and disturbances, in [12], robust stability and robust performance on tip tracking are expressed as the minimization of H_2/H_∞ norms of the augmented system, which is achieved by solving an optimization problem with the tool of Linear Matrix Inequality (LMI).

The above feedback control approaches may be adequate in dealing with disturbances and achieving good steady-state tracking accuracy. However, transient performances of the closed-loop systems are not clear for these feedback-based control strategies, especially for large tip movements. In reality, systems are often subject to a number of physical constraints, such as the input saturation limit of the actuator,

Manuscript received August 24, 2011. Accepted for publication January 30, 2012.

The work is supported in part by the Ministry of Education of China through a Chang Jiang Chair Professorship and in part by the US National Science Foundation (Grant No. CMMI-1052872). Corresponding author: Bin Yao.

Lu Lu (*lulu.lvlv@gmail.com*) and Bin Yao (*byao@ieee.org*) are with the State Key Laboratory of Fluid Power Transmission and Control of Zhejiang University in China as a visiting PhD student and a Chang Jiang Chair Professor respectively. They are also with the School of Mechanical Engineering, Purdue University, West Lafayette, USA. Zheng Chen (*cwlinus@gmail.com*), a student, and Qingfeng Wang (qfwang@zju.edu.cn), a professor, are with the State Key Laboratory of Fluid Power Transmission and Control of Zhejiang University, China.

the velocity constraints of the moving elements, and the allowable deflection range of the tip position of the flexible beam. Furthermore, the initial states of the system are sometimes very far away from the desired trajectory. To drive the states towards the desired trajectory as quickly as possible while satisfying all the constraints becomes a very difficult task that may not be achieved through pure feedback approaches alone. One has to resort to additional constrained optimization algorithms in order to solve the problem completely. A large class of control strategies such as optimal control and model predictive control[14], [15], [16], [17] do exist. However, the high complexity of these constrained optimization algorithms makes them implementable only with low sampling rate, which leads to poor disturbance rejection capability of the resulting closed-loop system. As a result, successful applications of these approaches to the precision motion control of mechanical systems are rare.

In this paper, the problem of tip position tracking control of the linear motor driven flexible beam with constraints and input disturbance is considered. The truncated mode method with clamped-mass boundary condition [6], [12] is firstly used to obtain the dynamic model of the Euler-Bernoulli beam. Overall dynamic equations of the system is then constructed by combining the above beam model with the 2rd-order model of the linear motor [18], [4]. Based on the model of the system, the novel two-loop control structure in [19] is generalized to achieve fast transient response with constraint satisfaction and good steady-state tracking accuracy simultaneously: a nonlinear feedback control law in continuous time domain in the inner-loop and a constrained optimization based trajectory replanning unit implemented in the discrete-time domain with the sampling rate chosen to account for the potential heavy computation in the outer loop. The proposed control strategy is also implemented on a HIWIN linear motor stage with a flexible beam attached to it. Comparative simulation and experimental results obtained demonstrate the effectiveness of the proposed approach in practical applications.

In sum, this paper develops a novel two-loop control strategy that may be extended to the control of more general flexible systems. By seamlessly incorporating an outer-loop online trajectory replanning unit into the feedback control structure as done in the paper, transient performance of the resulting closed-loop responses of the flexible system could be improved significantly when compared to the traditional feedback-based approaches.

II. Modeling of the System

Schematic diagram of the system under study is shown in Fig. 1. The beam is assumed to be a cantilever beam with uniformly distributed mass. One end of the beam is clamped to a stage having an inertia of M and the other end is rigidly attached to a tip load which is assumed to be a point mass of m and is free to move. The stage is powered by the electro-magnetic force $f(t)$ generated by a linear motor and is constrained to move along the Y-axis direction only. The motion of the system is in the horizontal plane, and thus the effect of gravity is ignored. Furthermore, since the beam deflection is very small when compared to the length of the beam, the axial motion of the flexible beam is ignored and only the lateral vibration of the beam is considered. Let $w(x,t)$ be the lateral displacement of the point on the beam having a distance of x to its base before the beam deflects. Then, the x-coordinate of the tip position shown in Fig. 1 is the same as the beam length L and its y-coordinate is represented by the lateral vibration of the beam at $x = L$. Let $p_b(t)$ and $p_e(t)$ be the position of the linear motor stage and the tip of the beam in the Cartesian coordinate OXY respectively. Then, $p_e(t) = p(L,t) = p_b(t) + w(L,t)$. The goal is to decide the control input signal $u(t)$ to be applied to the linear motor stage such that the tip position $p_e(t)$ reaches to any given position p_{ed} as fast as possible. It is noted that, though vibration of the beam is caused by the translational acceleration at the base, the control approach proposed in this paper can be easily extended to the case when the movement of the base is rotational.

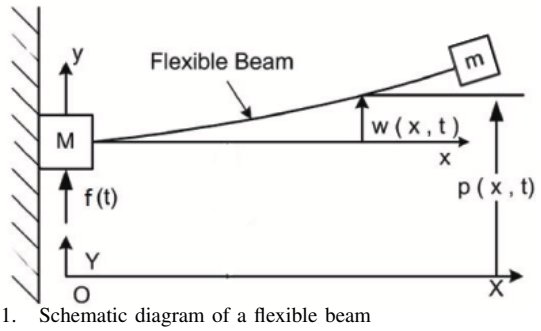

Figure 1. Schematic diagram of a flexible beam

Assuming that the flexible beam is very lightly damped, using the truncated mode method with clamped-mass boundary condition [6], [12], dynamic model of the system can be obtained as follows:

$$\begin{aligned}
&(\rho \int_0^L \varphi_i(x)\,dx + m\varphi_i(L))\ddot{p}_b(t) + \ddot{q}_i(t) + 2\xi_i\omega_i\dot{q}_i(t) \\
&+\omega_i^2 q_i(t) = 0, \quad i = 1,\cdots,\infty \\
&(M+m+\rho L)\ddot{p}_b(t) + \sum_{i=1}^{\infty}(\rho \int_0^L \varphi_i(x)\,dx + m\varphi_i(L))\ddot{q}_i(t) \\
&= kS(u) - b\dot{p}_b(t) - \Delta(t). \\
&w(x,t) = \sum_{i=1}^{\infty} \varphi_i(x) q_i(t)
\end{aligned} \tag{1}$$

where ρ is the linear density of the beam inertia, $\varphi_i(x)$ and q_i are the eigenfunction and the generalized coordinates of the i-th vibration mode of the beam deflection respectively, with $\xi_i \ll 1$ and ω_i being the damping ratio and the oscillating frequency of the mode, $f(t) = kS(u)$ represents the electro-magnetic force generated by the linear motor when ignoring the amplifier dynamics, in which k is the amplifier static gain, $u(t)$ is the input voltage, and $S(.)$ is the saturation function given by

$$S(u) = \begin{cases} u, & \text{if} \quad |u| \le u_M \\ u_M \text{sign}(u), & \text{if} \quad |u| > u_M, \end{cases} \tag{2}$$

where u_M denotes the input saturation limit. b represents the viscous friction coefficient of the stage system and $\Delta(t)$ denotes the lumped input disturbances and uncertainties such as the un-modeled nonlinear friction acting on the stage.

Let E and I be the Young's modulus and the moment of inertia of the cross section area with respect to the z-axis of the beam respectively. Then, the frequency ω_i and the eigenfunction $\varphi_i(x)$ of all modes are determined by [12]

$$\begin{array}{rl} \omega_i = & \sqrt{\frac{EI}{\rho}}\frac{\beta_i^2}{L^2} \\ \varphi_i(x) = & a_i[cosh(\frac{\beta_i}{L}x)-cos(\frac{\beta_i}{L}x) \\ & -\frac{cosh(\beta_i)+cos(\beta_i)}{sinh(\beta_i)+sin(\beta_i)}(sinh(\frac{\beta_i}{L}x)-sin(\frac{\beta_i}{L}x))] \end{array} \tag{3}$$

where β_is are all the positive solutions of

$$1+cos(\beta)cosh(\beta)+\frac{m\beta}{\rho L}[cos(\beta)sinh(\beta)-sin(\beta)cosh(\beta)]=0, \tag{4}$$

and a_is are nonzero constants determined from the normalization conditions

$$\int_0^L \rho\varphi_i(x)\varphi_i(x)\,dx+m\varphi_i(L)\varphi_i(L)=1 \tag{5}$$

In actual applications, only the first few modes need to be considered when the closed-loop bandwidth of the controller is limited below certain values. Suppose that only the first l modes need to be considered. Defining $\Delta_1(x,t)=\sum_{i=l+1}^{\infty}\varphi_i(x)q_i(t)$, $M_b=M+m+\rho L$ and $M_{qi}=\rho\int_0^L\varphi_i(x)dx+m\varphi_i(L)$, $\forall i=1,\cdots,\infty$, the truncated dynamical model of the flexible beam can be written in the following compact form:

$$\begin{array}{l} \left[\begin{array}{cc} \mathbf{I_{l\times l}} & \mathbf{M_q} \\ \mathbf{M_q^T} & M_b \end{array}\right]\left[\begin{array}{c} \ddot{\mathbf{q}} \\ \ddot{p}_b \end{array}\right]+\left[\begin{array}{cc} C_\xi & \mathbf{0_{l\times 1}} \\ \mathbf{0_{1\times l}} & b \end{array}\right]\left[\begin{array}{c} \dot{\mathbf{q}} \\ \dot{p}_b \end{array}\right] \\ +\left[\begin{array}{cc} K_\omega & \mathbf{0_{l\times 1}} \\ \mathbf{0_{1\times l}} & 0 \end{array}\right]\left[\begin{array}{c} \mathbf{q} \\ p_b \end{array}\right]=\left[\begin{array}{c} \mathbf{0_{l\times 1}} \\ kS(u)-\Delta(t)-\Delta_2(t) \end{array}\right], \\ w(x,t)=\sum_{i=1}^{l}\varphi_i(x)q_i(t)+\Delta_1(t), \end{array} \tag{6}$$

where

$$\begin{array}{l} \mathbf{q}=[q_1,\cdots,q_l]^T,\ \mathbf{M_q}=[M_{q1},\cdots,M_{ql}]^T, \\ C_\xi=diag\{2\xi_1\omega_1,\cdots,2\xi_l\omega_l\}, \\ K_\omega=diag\{\omega_1^2,\cdots,\omega_l^2\},\ \Delta_2(t)=\sum_{i=l+1}^{\infty}M_{qi}\ddot{q}_i(t) \end{array} \tag{7}$$

III. Problem Formulation

Let $\mathbf{x}=[q_1,\dot{q}_1,\cdots,q_l,\dot{q}_l,p_b,\dot{p}_b]^T$. Assuming that the high-order modes can be neglected (i.e., $\Delta_1(x,t)\approx 0$ and $\Delta_2(t)\approx 0$), the system (with input as $u(t)$ and output as $p_e(t)$) can then be represented in the following state-space form:

$$\begin{array}{rcl} \dot{\mathbf{x}} & = & \mathbf{A}\mathbf{x}+\mathbf{B}(S(u)+\Delta'(t)) \\ p_e & = & \mathbf{C}\mathbf{x}, \end{array} \tag{8}$$

where

$$\begin{array}{l} \mathbf{A}=\{a_{ij}\}_{(2l+2)\times(2l+2)},\ \mathbf{B}=\{b_i\}_{(2l+2)\times 1}, \\ \mathbf{C}=[\varphi_1(L),0,\cdots,\varphi_l(L),0,1,0], \\ \Delta'(t)=-\frac{\Delta(t)}{M_b-\sum_{j=1}^{l}M_{qi}^2}. \end{array} \tag{9}$$

The coefficients of $\mathbf{A}$ and $\mathbf{B}$ are computed as follows:

$$\left\{\begin{array}{l} a_{2i-1,2i}=1,\ \forall i=1,\cdots,l+1; \\ a_{2l+2,2i-1}=\frac{M_{qi}\omega_i^2}{M_b-\sum_{j=1}^{l}M_{qj}^2},\ \forall i=1,\cdots,l; \\ a_{2l+2,2i}=\frac{2M_{qi}\xi_i\omega_i}{M_b-\sum_{j=1}^{l}M_{qj}^2},\ \forall i=1,\cdots,l; \\ a_{2l+2,2l+2}=\frac{-b}{M_b-\sum_{j=1}^{l}M_{qj}^2}; \\ a_{2i,2i-1}=-M_{qi}a_{2l+2,2i-1}-\omega_i^2,\ \forall i=1,\cdots,l; \\ a_{2i,2i}=-M_{qi}a_{2l+2,2i}-2\xi_i\omega_i,\ \forall i=1,\cdots,l; \\ a_{2i,2j-1}=-M_{qi}a_{2l+2,2j-1}, \\ \quad \forall i=1,\cdots,l,\ j=1,\cdots,i-1,i+1,\cdots,l; \\ a_{2i,2j}=-M_{qi}a_{2l+2,2j}, \\ \quad \forall i=1,\cdots,l,\ j=1,\cdots,i-1,i+1,\cdots,l; \\ a_{2i,l+2}=-M_{qi}a_{2l+2,2l+2},\ \forall i=1,\cdots,l; \\ a_{i,j}=0,\ \text{for other } i,j\le 2l+2. \end{array}\right. \tag{10}$$

$$\left\{\begin{array}{l} b_{2i-1}=0,\ \forall i=1,\cdots,l+1; \\ b_{2l+2}=\frac{k}{M_b-\sum_{j=1}^{l}M_{qj}^2}; \\ b_{2i}=-M_{qi}b_{2l+2}\ \forall i=1,\cdots,l. \end{array}\right.$$

It is easy to verify that the pair $(\mathbf{A},\mathbf{B})$ is controllable. The system is assumed to have the following state constraints:

$$\mathbf{x}\in\mathscr{X}, \tag{11}$$

where $\mathscr{X}\triangleq\{\mathbf{x}: x_{imin}\le x_i\le x_{imax}\}$ is a bounded convex set in R^{2l+2} whose bounds incorporates the information of the position and velocity constraints of the base and the maximum deflection constraints of the flexible beam.

Assumption 1: There exists a known constant d such that

$$|\Delta'(t)|\le d<u_M \tag{12}$$

The above assumption states that the maximum level of the unknown input disturbance must be less than the input saturation limit so that it is possible to design an input control law within the saturation limit to suppress the disturbance. It is also assumed that the values of all the generalized coordinates $q_1,\dot{q}_1,\cdots,q_l,\dot{q}_l$, the position and velocity of the linear motor are available for the design of feedback control law. Optical devices, strain gauges, vision systems or real-time observers [20] can be used to directly or indirectly obtain the values of q_is and their derivatives.

The reference tracking problem is considered in this paper. The objective is to design a control law $u(t)$ such that the output $p_e(t)$ converges to the constant desired output p_{ed} as fast as possible and the tracking error $e_d(t)=p_e(t)-p_{ed}$ at the steady state is as small as possible while the constraints (11) are not violated all the time. For the desired reference p_{ed} to be trackable, there exists $\mathbf{x_d}=[0,\cdots,0,p_{bd},0]^T$ such that $p_{bd}=p_{ed}$, where $\mathbf{x_d}$ satisfies the following assumptions

Assumption 2:

$$\mathbf{x_d}\in\mathscr{X}', \tag{13}$$

where $\mathscr{X}'\triangleq\{\mathbf{x}': x'_{imin}\le x'_i\le x'_{imax}\}$ is a convex set contained in the interior of $\mathscr{X}$, i.e., $x'_{imin}>x_{imin}$, $x'_{imax}<x_{imax}$.

Remark 1: Assumption 2 requires that the valid region for the desired setpoint (and for the replanned trajectory to be

synthesized in the future as well) $\mathscr{X}'$ should be smaller than the region $\mathscr{X}$. The margin is left for the tracking error.

IV. Overall Controller Structure

It is seen from the above section that two objectives - fast transient converging speed under the constraints of the system and good steady state tracking accuracy - need to be met simultaneously. In the following, similar to [19], a two-loop control structure shown in Fig. 2 is developed to solve the problem and is outlined below:

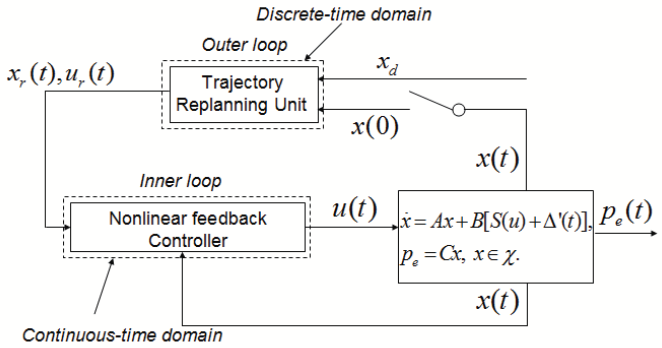

Figure 2. Overall control structure.

- In the inner loop, a trajectory tracking controller that explicitly takes into account the constraints of the system to achieve a guaranteed output tracking performance even in the presence of disturbances is designed and implemented in continuous-time domain. Specifically, as long as the states of the tracking error dynamics with respect to the replanned trajectory $p_{er}(t)$ are within a pre-specified region Ω at certain time instance, the tracking error dynamics will stay inside Ω thereafter in spite of the disturbances assumed in (12) and exponentially converge to zero when the disturbances disappear, assuming that the replanned trajectory satisfies certain conditions set forth.
- In order to prevent constraints violation from happening when the initial states of the tracking error dynamics with respect to the desired target $\mathbf{x_d}$ are large, the reference trajectory actually fed into the inner trajectory tracking controller, i.e., $p_{er}(t)$, is replanned such that (i) the initial states of the tracking error dynamics with respect to $\mathbf{x_r}$ are always within Ω, (ii) $p_{er}(t)$ satisfies all the conditions set forth in the design of inner trajectory tracking controller, and (iii) $p_{er}(t)$ converges to p_{ed} as quickly as possible for a fast overall response speed. It should be noted that, the replanned trajectory to be generated contains not only $p_{er}(t)$, but also the corresponding $\mathbf{x_r}(t)$ and $u_r(t)$. Specific trajectory replanning algorithms that accomplish these objectives will be developed and implemented in discrete-time domain using relatively low sampling rate of $1/T$ to accommodate the potential computation burden in solving the posted constrained optimization problem.

V. Design of Inner-loop Controller

Suppose that the replanned trajectory $p_{er}(t)$ to be synthesized in the outer loop satisfies the following dynamic equations:

$$\begin{aligned} \dot{\mathbf{x}}_\mathbf{r} &= \mathbf{A}\mathbf{x_r} + \mathbf{B}u_r \\ p_{er} &= \mathbf{C}\mathbf{x_r}, \end{aligned} \tag{14}$$

where $\mathbf{x_r}$ is the time-varying state of replanned trajectory, and u_r is the time-varying input of the replanned trajectory. Defining $\mathbf{z_r} = \mathbf{x} - \mathbf{x_r}$ to be the vector of tracking error and $e_r = p_e - p_{er}$ to be the output tracking error with respect to the replanned trajectory, the tracking error dynamics is then represented by

$$\begin{aligned} \dot{\mathbf{z}}_\mathbf{r} &= \mathbf{A}\mathbf{z_r} + \mathbf{B}[S(u) - u_r + \Delta'(t)], \\ e_r &= \mathbf{C}\mathbf{z_r}. \end{aligned} \tag{15}$$

Let the control law be

$$u = u_r - \sigma(\mathbf{K}\mathbf{z_r}), \tag{16}$$

where $\mathbf{K}$ is the vector of feedback gain such that the matrix $\mathbf{A} - \mathbf{B}\mathbf{K}$ is Hurwitz, and the nonlinear function $\sigma(\mathbf{K}\mathbf{z_r})$ is defined by

$$\sigma(\mathbf{K}\mathbf{z_r}) = \begin{cases} \mathbf{K}\mathbf{z_r}, & \text{if } \mathbf{z_r^T}\mathbf{P}\mathbf{z_r} \le c_1, \\ \frac{(\mathbf{z_r^T}\mathbf{P}\mathbf{z_r} - c_1)\sigma_1(z_r)}{c_2 - c_1} + \frac{(c_2 - \mathbf{z_r^T}\mathbf{P}\mathbf{z_r})\mathbf{K}\mathbf{z_r}}{c_2 - c_1}, \\ \text{if } c_1 < \mathbf{z_r^T}\mathbf{P}\mathbf{z_r} \le c_2, \end{cases} \tag{17}$$

in which c_1 and c_2 are two positive numbers with $c_2 > c_1$. $\mathbf{P}$ is the positive definite solution of the Lyapunov equation $(\mathbf{A^T} - \mathbf{K^T}\mathbf{B^T})\mathbf{P} + \mathbf{P}(\mathbf{A} - \mathbf{B}\mathbf{K}) = -\mathbf{Q}$ where $\mathbf{Q}$ is some positive definite matrix. The function $\sigma_1(z_r)$ is defined by

$$\sigma_1(\mathbf{z_r}) = \begin{cases} 0, & \text{if } \mathbf{z_r^T}\mathbf{P}\mathbf{B} = 0 \text{ or } \frac{\mathbf{z_r^T}\mathbf{Q}\mathbf{z_r}}{2|\mathbf{z_r^T}\mathbf{P}\mathbf{B}|} \ge d + \varepsilon, \\ \left(d + \varepsilon - \frac{\mathbf{z_r^T}\mathbf{Q}\mathbf{z_r}}{2|\mathbf{z_r^T}\mathbf{P}\mathbf{B}|}\right) \cdot \text{sign}(\mathbf{z_r^T}\mathbf{P}\mathbf{B}), & \text{else.} \end{cases} \tag{18}$$

where ε is a positive constant such that $u_M - d - \varepsilon > 0$. It is easily checked that $\sigma_1(\mathbf{z_r})$ is continuous everywhere in R^{2l+2} except for the origin. Thus, the nonlinear function $\sigma(\mathbf{K}\mathbf{z_r})$ is always continuous.

In the above control law, the nonlinear feedback term $\sigma(\mathbf{K}\mathbf{z_r})$ has two regions. The linear region with $\mathbf{z_r^T}\mathbf{P}\mathbf{z_r} \le c_1$ represents the normal operation of the system with $\mathbf{K}$ properly selected to meet the disturbance rejection performance requirement at the steady-state while not being overly large to avoid potential implementation problems such as the severe sensitivity to noise at the steady-state and the excitation of neglected high-frequency dynamics. The nonlinear region with $c_1 \le \mathbf{z_r^T}\mathbf{P}\mathbf{z_r} \le c_2$ has a higher feedback term, which is to make sure that when the tracking error is about to go out of the region defined by $\Omega = \{\mathbf{z_r} : \mathbf{z_r^T}\mathbf{P}\mathbf{z_r} \le c_2\}$, large enough control effort will be generated to pull the tracking error back. With this control law, the set Ω is a positive invariant set, i.e., once the $\mathbf{z_r}$ is within this positive invariant set, it will not go out of this set any more, as detailed in the following lemma:

Lemma 1: With the control law (16), the set $\Omega = \{\mathbf{z_r} : \mathbf{z_r^T}\mathbf{P}\mathbf{z_r} \le c_2\}$ is a positive invariant set and (11) is always

satisfied $\forall \mathbf{z_r} \in \Omega$ if the following conditions are satisfied:

$$\begin{array}{l} c_2 < \frac{\varepsilon^2}{\mathbf{KP^{-1}K^T}}, \\ |u_r| \le u_M - d - \varepsilon, \\ \sqrt{c_2 \mathbf{z_i'} \mathbf{P^{-1}} \mathbf{z_i'^T}} \le \min\{x_{imax} - x'_{imax}, x'_{imin} - x_{imin}\}, \\ \quad \forall i = 1, \cdots, 2l+2, \\ \mathbf{x_r} \in \mathscr{X}'. \end{array} \tag{19}$$

In the above, $\mathbf{z_i'} = [0, \cdots, 0, \underbrace{1}_{i}, 0, \cdots, 0]$.

Proof: A simple calculation shows that within the ellipse $\mathbf{z_r^T P z_r} \le c_2$, the maximum value of $|\mathbf{Kz_r}|$ is bounded by $\sqrt{c_2}\sqrt{\mathbf{KP^{-1}K^T}}$. Thus, the 1st inequality of (19) guarantees that $|\mathbf{Kz_r}| < \varepsilon < d + \varepsilon \le u_M - u_r$. Furthermore, $|\sigma_1(\mathbf{z_r})| \le d + \varepsilon \le u_M - u_r$. Thus, from the expression (17), it is obvious that $|\sigma(\mathbf{Kz_r})| \le u_M - u_r$, which means that the input $u = u_r - \sigma(\mathbf{Kz_r})$ never saturates within Ω, i.e., $S(u) = u$. The tracking error dynamics can then be represented as

$$\begin{array}{rcl} \dot{\mathbf{z}}_\mathbf{r} &=& \mathbf{A z_r} + \mathbf{B}[-\sigma(\mathbf{Kz_r}) + \Delta'(t)], \\ e_r &=& \mathbf{C z_r}. \end{array} \tag{20}$$

Furthermore, a simple calculation also shows that $\sqrt{c_2 \mathbf{z_i'} \mathbf{P^{-1}} \mathbf{z_i'^T}}$ is the maximum absolute value of i-th coordinate for all the points inside the ellipse $\mathbf{z_r^T P z_r} \le c_2$. From the 3rd inequality of (19), the tracking error in each dimension is always within the margin between $\mathscr{X}$ and $\mathscr{X}'$. Thus, the 4th inequality of (19) guarantees that the state constraints are never violated.

Define $V(\mathbf{z_r}) = \mathbf{z_r^T P z_r}$. To prove that $\Omega = \{\mathbf{z_r} : V(\mathbf{z_r}) \le c_2\}$ is a positive invariant set, it is sufficient to check that $\dot{V} < 0$ on the boundary of Ω, $\partial\Omega = \{\mathbf{z_r} : V(\mathbf{z_r}) = c_2\}$. To show this, first notice that $\sigma(\mathbf{Kz_r}) = \sigma_1(\mathbf{z_r})$ on $\partial\Omega$. Thus, on $\partial\Omega$, we have the following two cases:

Case 1 : $\mathbf{z_r^T PB} = 0$ or $\frac{\mathbf{z_r^T Q z_r}}{2|\mathbf{z_r^T PB}|} \ge d + \varepsilon$

In this case,

$$\begin{array}{rl} \dot{V} & = \mathbf{z_r^T}(\mathbf{A^T P + PA})\mathbf{z_r} + 2\mathbf{z_r^T PB}[-\sigma_1(\mathbf{z_r}) + \Delta'(t)] \\ & = -\mathbf{z_r^T Q z_r} + 2\mathbf{z_r^T PB}[\mathbf{Kz_r} - \sigma_1(\mathbf{z_r}) + \Delta'(t)] \\ & \le -\mathbf{z_r^T Q z_r} + 2|\mathbf{z_r^T PB}|[\mathbf{Kz_r} + d]. \end{array} \tag{21}$$

① When $\mathbf{z_r^T PB} = 0$, $\dot{V} \le -\mathbf{z_r^T Q z_r} < 0$.

② When $\mathbf{z_r^T PB} \ne 0$, since $|\mathbf{Kz_r}| < \varepsilon$ in Ω, it follows that $\dot{V} < -\mathbf{z_r^T Q z_r} + 2|\mathbf{z_r^T PB}|[\varepsilon + d] \le 0$.

Case 2 : If $\frac{\mathbf{z_r^T Q z_r}}{2|\mathbf{z_r^T PB}|} < d + \varepsilon$

In this case, noticing that $|\mathbf{Kz_r}| < \varepsilon$ in Ω:

$$\begin{array}{rl} \dot{V} & = -\mathbf{z_r^T Q z_r} + 2\mathbf{z_r^T PB}[\mathbf{Kz_r} - \sigma_1(\mathbf{z_r}) + \Delta'(t)] \\ & = -2|\mathbf{z_r^T PB}|(d + \varepsilon) + 2\mathbf{z_r^T PB}[\mathbf{Kz_r} + \Delta'(t)] \\ & < 0. \end{array} \tag{22}$$

Thus, $\dot{V} < 0$ for all the points on $\partial\Omega$, which completes the proof. ■

Lemma 2: Inside Ω, the steady-state output tracking error (with respect to the replanned trajectory) $e_r = p_e - p_{er}$ is bounded above by $|e_r(\infty)| \le \sqrt{\min(c_2, c_3)}\sqrt{\mathbf{CP^{-1}C^T}}$, where $c_3 = \frac{4\lambda_{max}(\mathbf{P})\mathbf{B^T P Q^{-2} P B} d^2}{\lambda_{min}(\mathbf{Q})}$.

Proof: It can be checked out that, $\forall c > 0$, the maximum value of $|e_r| = |\mathbf{Cz_r}|$ within the ellipse set $\Omega_c = \{\mathbf{z_r} : V(\mathbf{z_r}) \le c\}$ is bounded by $\sqrt{c}\sqrt{\mathbf{CP^{-1}C^T}}$. It is thus obvious that the lemma is true if the level function V stays within $\min(c_2, c_3)$ at steady state. When $c_3 \ge c_2$, as Ω is a positive invariant set by Lemma 1, $V \le c_2 = \min(c_2, c_3)$ which shows that the lemma is true. When $c_3 < c_2$, we show in the following that $\dot{V} < 0$ for all the points in Ω with $c_3 < V \le c_2$:

- 1) If $\sigma(\mathbf{Kz_r})$ takes the value of $\mathbf{Kz_r}$, then

$$\begin{array}{rcl} \dot{V} &=& \mathbf{z_r^T}(\mathbf{A^T P + PA})\mathbf{z_r} + 2\mathbf{z_r^T PB}[-\mathbf{Kz_r} + \Delta'(t)] \\ &=& -\mathbf{z_r^T Q z_r} + 2\mathbf{z_r^T PB}\Delta'(t) \\ &\le& -\frac{1}{2}\mathbf{z_r^T Q z_r} + 2\Delta'(t)\mathbf{B^T P Q^{-2} P B}\Delta'(t) \\ &\le& -\frac{1}{2}\mathbf{z_r^T Q z_r} + 2\mathbf{B^T P Q^{-2} P B}d^2 \\ &\le& -\frac{\lambda_{min}(\mathbf{Q})}{2\lambda_{max}(\mathbf{P})}\mathbf{z_r^T P z_r} + 2\mathbf{B^T P Q^{-2} P B}d^2 \\ &<& 0 \end{array} \tag{23}$$

- 2) If $\sigma(\mathbf{Kz_r})$ takes the value of $\sigma_1(\mathbf{z_r})$, the proof that $\dot{V} < 0$ is similar to that in Lemma 1. Specifically, it can be seen from the two cases in the proof of Lemma 1 that the fact $\dot{V} < 0$ is true not only for all the points $\mathbf{z_r}$ on the boundary $\partial\Omega = \{\mathbf{z_r} : V(\mathbf{z_r}) = c_2\}$, but also for all the points $\mathbf{z_r}$ with $c_3 < V(\mathbf{z_r}) \le c_2$.

From (17), the function $\sigma(\mathbf{Kz_r})$ is either $\mathbf{Kz_r}$ or some value between $\mathbf{Kz_r}$ and $\sigma_1(\mathbf{z_r})$. It is thus easy to show that $\dot{V} < 0$ for all the points in Ω with $c_3 < V \le c_2$.

The proof is thus complete. ■

Remark 2: In order to better deal with the constant portion of input disturbances, an integrator with saturation limit can be introduced to the control law through the use of discontinuous-projection-based adaptation law for constant input disturbances as in [21], [22], [23]. The modified control law u is then given by

$$u = u_r - \sigma(\mathbf{Kz_r}) - \hat{\Delta}, \tag{24}$$

where the integration term $\hat{\Delta}$ is updated by [24], [25]:

$$\dot{\hat{\Delta}} = Proj_{\hat{\Delta}}(2\gamma \mathbf{z_r^T PB}) \tag{25}$$

in which $\gamma > 0$ is an arbitrary positive value and the projection mapping $Proj_{\hat{\Delta}}(\bullet)$ is defined as

$$Proj_{\hat{\Delta}}(\bullet) = \begin{cases} 0 & \text{if } \hat{\Delta} = d \text{ and } \bullet > 0 \\ 0 & \text{if } \hat{\Delta} = -d \text{ and } \bullet < 0 \\ \bullet & \text{otherwise} \end{cases} \tag{26}$$

Since the maximum absolute value of the term $\hat{\Delta}$ is d, the disturbance estimation error $\tilde{\Delta} = \hat{\Delta} - \Delta$ is bounded by $2d$. Thus, only the $'d'$ in (18) needs to be replaced by $'2d'$ should the modified control law (24) is used.

Combining proofs of the above two lemmas with properties of the discontinuous-projection-based adaptation law [21], [24], [25], it can be shown that with the modified control law (24), Lemma 1 and Lemma 2 are still true. Furthermore, if the disturbance term Δ is constant, we can define a new Lyapunov function $V_a = V + \frac{1}{2\gamma}\tilde{\Delta}^2$ and prove the asymptotic output tracking at steady state. These proofs are technically complicated in details and are thus omitted here for simplicity. In the experiment section later, the modified control (24) will be used and its effectiveness will be shown through the excellent experimental results obtained. △

Remark 3: In this paper, the inner-loop controller is designed based on the truncated-mode model of the flexible beam system. However, the stability of the system may be affected by the ignored high-order mode of the flexible beam vibration if the controller gains are not properly selected, which is known as "spillover problem" [26]. To avoid this problem, the first $2l$ elements of the gain vector K representing the feedback gains on the generalized coordinates of the first l modes should be chosen small enough such that the bandwidth of the closed-loop system is sufficiently low to avoid the excitation of the ignored high-frequency vibration modes.

In order for (19) to be satisfied, the following controller parameter selection procedure is proposed:

- Step 1: Choose K such that the closed-loop poles (the eigenvalues of $A-BK$) are properly assigned and the steady-state output tracking performance is met according to Lemma 2. Compute the corresponding P by solving the Lyapunov equation.
- Step 2: Choose $\varepsilon > 0$ such that $u_M - d - \varepsilon > 0$.
- Step 3: Choose c_1 and c_2 to be two positive constants such that $c_2 < \min\left[\frac{\varepsilon^2}{\mathbf{K}\mathbf{P}^{-1}\mathbf{K}^{\mathbf{T}}}, \frac{[\min(x_{imax}-x'_{imax}, x'_{imin}-x_{imin})]^2}{\mathbf{z}'_{\mathbf{i}}\mathbf{P}^{-1}\mathbf{z}'^{\mathbf{T}}_{\mathbf{i}}}\right]$ and $c_1 < c_2$.

It is easy to verify that, if the replanned trajectory $y_r(t)$ is chosen such that

$$\begin{array}{l} |u_r(t)| \le u_M - d - \varepsilon, \\ \mathbf{x_r}(t) \in \mathscr{X}' \end{array} \tag{27}$$

then the above design procedure guarantees that all the inequalities in (19) are satisfied. Thus, noting that arbitrarily good disturbance rejection performance has been achieved inside the set Ω with the above design procedure, all the three objectives stated at the beginning of this section will be met simultaneously if the reference trajectory $p_{er}(t)$ is generated in such a way that it converges to the desired target p_{ed} fast enough while satisfying (27) and keeping the initial tracking errors $\mathbf{z_r}(0)$ within Ω for the initial states of the system $\mathbf{x_r}(0)$. Such a trajectory replanning design is given in the next section.

VI. Trajectory Replanning

The outer loop implements an online trajectory replanning algorithm when the initial state $\mathbf{x}(0)$ is far away from the desired target $\mathbf{x_d}(t)$.

Set $\mathbf{x_r}(0) = \mathbf{x}(0)$ so that $\mathbf{z_r}(0) = \mathbf{0} \in \Omega$. Then, the following constrained optimization problem needs to be solved so that the constraints (27) are satisfied and the replanned trajectory converges to the desired target as fast as possible:

$$\begin{array}{c} \min\limits_{u'_r(t),\ t\in[0,\ t_f]} t_f \quad \text{subject to} \\ \mathbf{x_r}'(0) = \mathbf{x_r}(0), \\ \mathbf{x_r}'(t_f) = \mathbf{x_d}, \\ \dot{\mathbf{x_r}}'(t) = \mathbf{A}\mathbf{x'_r}(t) + \mathbf{B}u'_r(t), \\ |u'_r(t)| \le u_M - d - \varepsilon, \\ \mathbf{x_r}'(t) \in \mathscr{X}',\ \forall t \ge 0. \end{array} \tag{28}$$

It may take some time to solve the above constrained optimization problem, which makes it difficult to implement the algorithm online at a high-sampling rate. However, since the disturbance rejection performance goal has already been met by the inner loop controller in continuous-time domain, it is not necessary to use high-sampling rate in the outer loop to generate the replanned trajectory. The sampling period for the outer loop can be selected to be long enough to take into account the heavy computational burden when solving the constrained optimization problem (28) on-line.

Besides explicitly solving the constrained optimization algorithm (28) online, a more efficient algorithm that employs the offline pre-parametrization of the optimal trajectory can be used as follows. It is seen that, when the constraints $|u'_r(t)| \le u_M - d - \varepsilon$ and $\mathbf{x_r}'(t) \in \mathscr{X}'$ are fixed, the optimal solution $u^*_r(t)$ of the above problem only depends on the initial states $\mathbf{x_r}(0)$ and the target output p_{ed}. Thus, one can first solve the problem (28) off-line with various initial conditions in the region $\mathscr{X}'$ and output targets p_{ed}, and then parameterize the optimal solution $u^*_r(t)$ as a function of the initial states and the desired target. The parametrized optimal solutions are subsequently stored into the memory so that in online implementation, only a simple evaluation procedure is executed every time T to fetch the optimal solution $u^*_r(t)$ to be applied in the future. This algorithm is detailed as follows:

- Offline: Solve the problem

$$\begin{array}{c} \min\limits_{u'_r(t),\ t\in[t_0,\ t_f]} t_f \quad \text{subject to} \\ \mathbf{x_r}'(t_0) = \mathbf{v_1}, \\ \mathbf{x_r}'(t_f) = [0\cdots,0,\cdots,v_2,0]^T, \\ \dot{\mathbf{x}}_{\mathbf{r}}'(t) = \mathbf{A}\mathbf{x'_r}(t) + \mathbf{B}u'_r(t), \\ |u_r(t)'| \le u_M - d - \varepsilon, \\ \mathbf{x_r}' \in \mathscr{X}',\ \forall t \ge 0, \end{array} \tag{29}$$

  for various $\mathbf{v_1} \in \mathscr{X}'$ and $p'_{bmin} \le v_2 \le p'_{bmax}$, where p'_{bmin} and p'_{bmax} are the lower and upper bounds of the projection of $\mathscr{X}'$ onto the p_b-axis.

  The optimal solution in the future time T period, i.e., $u^*_r(t),\ t \in [t_0, t_0+T]$, is thus a function of $\mathbf{v_1}$ and v_2. This function, denoted as $f(\mathbf{v_1}, v_2)$, is obtained in the offline computation and saved into the memory for the online use.
- Online:
  - Initialization: Set $u_r(t) = 0,\ \forall t \in [0, T]$.
  - During the time period $[kT, (k+1)T]$, $k \ge 0$:

    1) Solve the following linear differential equation with initial condition $\mathbf{x_r}(kT)$ to obtain $\mathbf{x_r}(t),\ \forall t \in [kT, (k+1)T]$:

$$\dot{\mathbf{x}}_{\mathbf{r}}(t) = \mathbf{A}\mathbf{x_r}(t) + \mathbf{B}u_r(t). \tag{30}$$

    The obtained $\mathbf{x_r}(t)$ is fed into the inner-loop tracking controller together with $u_r(t)$ as the replanned trajectory.

    2) Plug in the values of $\mathbf{x_r}((k+1)T)$ and p_{ed} into the function f to obtain the optimal $u_r(t)$ during the next sampling period, i.e.,

$$\underset{t\in[(k+1)T,(k+2)T]}{u_r(t)} = f(\mathbf{x_r}((k+1)T), p_{ed}) \tag{31}$$

Denote $\mathscr{X}_c \subset \mathscr{X}$ as the set of all initial conditions $\mathbf{x_r}(t)$ such that the problem (28) is feasible. It is obvious that, if $\mathbf{x_r}(t) = exp(\mathbf{A}t)\mathbf{x_r}(0) \in \mathscr{X}_c, \forall t \in [0, T]$, then $u_r(t)$ generated from the

above on-line algorithm will be the same as the off-line time-optimal solution in (29) with $t_0 = T$ and $\mathbf{v_1} = exp(\mathbf{A}T)\mathbf{x_r}(0)$, which definitely drives $\mathbf{x_r}$ towards zero in a finite time.

In actual implementation, the original system can be discretized and multi-parametric programming technique [16], [27] can be applied to solve the problem (29) offline and parameterize the optimal solution as a piecewise affine function of the states and desired target with each definition region being a polytope inside $\mathscr{X}'$. Commercial tools for solving this type of problems are available [28].

It should be noted that in the offline part of the algorithm, "Solving the problem (29) for various $\mathbf{v_1} \in \mathscr{X}'$ and $p'_{bmin} \le v_2 \le p'_{bmax}$" does not literally mean that one has to really evaluate all the possible initial conditions and desired target. Actually, as detailed in the book on multi-parametric programming [16], the overall parameterized optimal control law is a function of the initial conditions and desired target that consists of only finite number of pieces. Each piece of this function has one simple expression only. Thus, it is only necessary to pick up some finite number of initial states and desired targets to solve for the overall parameterized control law without any degradation of the accuracy.

Remark 4: It is seen that the set $\mathscr{X}_c$ determines the "maximum domain of attraction" of the desired state $\mathbf{x_d}$ under the dynamic constraint $\dot{\mathbf{x}}_\mathbf{r}'(t) = \mathbf{A}\mathbf{x}'_\mathbf{r}(t) + \mathbf{B}u'_r(t)$, the input constraint $|u'_r(t)| \le u_M - d - \varepsilon$ and the state constraints $\mathbf{x_r}'(t) \in \mathscr{X}'$. If $\mathbf{x_r}(T) = exp(\mathbf{A}T)\mathbf{x_r}(0) \in \mathscr{X}_c$, the time-optimal solution of problem (29) exists and can be computed by the proposed algorithm. Theoretically, it is very difficult to quantify the exact size of $\mathscr{X}_c$ because of various types of constraints of the systems. However, in actual implementation, after the original system is discretized, $\mathscr{X}_c$ can be easily computed by using the polytope algorithms in [28]. The size of $\mathscr{X}_c$ is generally very large and contains the actual states of the system in almost all the cases. Thus, the existence of the solution for (28) and (29) will not be a serious problem in actual implementation.

VII. Theoretical Result

Noting Lemmas 1 and 2 with properties of the trajectory replanning algorithm, the following theoretical results are obtained for the proposed two-loop control structure strategy:

Theorem 1: Consider the inner-loop trajectory tracking control law (16) with all the controller parameters chosen by Steps 1 to 3 and the reference trajectories generated on-line through the outer-loop trajectory replanning algorithm given in section VI. Then, when $\mathbf{x_r}(t) = exp(\mathbf{A}t)\mathbf{x_r}(0) \in \mathscr{X}_c, \forall t \in [0,T]$, the state tracking error with respect to the desired target ($\mathbf{z_d} = \mathbf{x} - \mathbf{x_d}$) converges to Ω in a finite time, and the constraints (11) are always satisfied. Furthermore, the steady-state output tracking error $e_d(\infty)$ (with respect to the desired setpoint p_{ed}) is bounded by $\sqrt{\min(c_2,c_3)}\sqrt{\mathbf{C}\mathbf{P}^{-1}\mathbf{C}^\mathbf{T}}$.

VIII. Experiments

A. Experimental Setup

The same single-axe commercial stage by HIWIN set-up in the Precision Mechatronics Laboratory at Zhejiang University as in [29] is used. The stage is powered by an epoxy-core linear motor and has a travel distance of $0.51m$. The maximum allowable traveling speed of the stage is approximately $2m/s$. Linear encoder is used with a position measurement resolution of $0.5\mu m$. An aluminum-made flexible beam is clamped on the stage and stretches out in the direction perpendicular to the direction of motion of the stage. The tip position is measured by a Renishaw laser interferometer with a measurement resolution of $0.5\mu m$. The velocity signals of the base and the tip are obtained by directly differentiating the position signals in discrete-time domain with a sampling rate of $5kHz$. The entire system, graphically shown in Fig. 3, is used as the motion system hardware for the study. To implement real-time control algorithm, the above system is connected to a dSPACE CLP1103 controller board. The maximum input voltage sent from controller is $10V$.

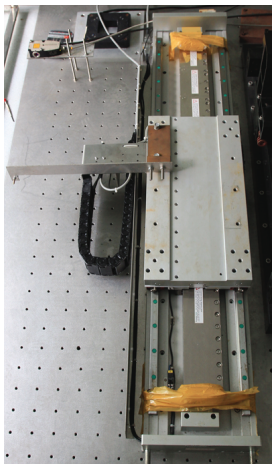

Figure 3. System setup.

B. System Identification

As in [29], dynamics of the linear motor stage before the beam is attached to it can be described by a second-order system given by

$$M\ddot{p}_b = kS(u) - b\dot{p}_b + \Delta(t). \tag{32}$$

The amplifier gain $k = 45N/V$ and $M = 15kg$ is obtained from the manual of the linear motor driven stage. Then a simple least-square identification procedure is done to estimate the normalized inertia friction coefficient b/k, from which the estimate of b is obtained to be $32N \cdot s/m$. Since there is no cogging force effect for the epoxy core motor, the term $\Delta(t)$ is relatively small. The bound d for the normalized disturbance $\Delta(t)/(M+m+\rho L)$ is taken as $100N/kg$. The input saturation limit $u_M = 10V$.

The beam used in the experiment has a rectangular cross section with the width $l_w = 3.98 \times 10^{-2}m$ and the thickness $l_t = 2.4 \times 10^{-3}m$. Thus, $I = \frac{1}{12}l_w l_t^3 = 4.585 \times 10^{-11}m^4$. Other parameters of the beam are: $L = 0.4m$, $E = 71.7 \times 10^9 N/m^2$, $\rho = 2.7 \times 10^3 kg/m^3 \cdot l_w \cdot l_t$. Since the tip mass is a piece of reflection mirror with super light weight, m is taken as 0. And the values of ξ_is are chosen to be zero because the damping of the beam is too low. All the other parameters of the system

can be calculated from the above values. The deflection of the beam w is obtained by subtracting the measured base position from the measured tip position. The Bode magnitude plot of the transfer function from the base position y to the tip deflection w is also obtained and shown in Fig. 4. It is seen that the natural frequencies of the first several vibration modes of the beam are $72.5rad/s$, $490rad/s$, $1567rad/s$, which are somewhat different from the values calculated from the theoretical parameters, showing that the system may have certain modeling uncertainties and parametric uncertainties. Nominal values of the natural frequencies are then taken to be the ones obtained from the Bode magnitude plot.

It is possible to use observers to estimate q_is from the tip position w. However, such a scheme is sensitive to the modeling error of the beam and may be subject to significant side effects caused by various types of disturbances of the system. Thus, we consider only the first vibration mode and ignore all the higher order modes. With this simplification, the resulting system is of fourth order, and $q_1(t) = \frac{w(t)}{\varphi_1(L)}$, $\dot{q}_1(t) = \frac{\dot{w}(t)}{\varphi_1(L)}$. It must be kept in mind that the obtained q_1 and $\dot{q}_1$ actually contains the higher-order modes effects. Thus, when designing the feedback controller, the feedback gains on q_1 and $\dot{q}_1$ should be chosen to be sufficiently low so that the high-order dynamics are not excited to cause adverse effects.

The bounds for $\mathscr{X}$ are as follows: $x_{1min} = -\frac{0.005}{\varphi_1(L)}m$, $x_{1max} = \frac{0.005}{\varphi_1(L)}m$, $x_{2min} = -\frac{0.08}{\varphi_1(L)}m/s$, $x_{2max} = \frac{0.08}{\varphi_1(L)}m/s$, $x_{3min} = -0.05m$, $x_{3max} = 0.45m$, $x_{4min} = -2.05m/s$, $x_{4max} = 2.05m/s$. And the bounds for $\mathscr{X}'$ are as follows: $x'_{1min} = -\frac{0.0048}{\varphi_1(L)}m$, $x'_{1max} = \frac{0.0048}{\varphi_1(L)}m$, $x'_{2min} = -\frac{0.05}{\varphi_1(L)}m/s$, $x'_{2max} = \frac{0.05}{\varphi_1(L)}m/s$, $x'_{3min} = -0.01m$, $x'_{3max} = 0.41m$, $x'_{4min} = -2m/s$, $x'_{4max} = 2m/s$.

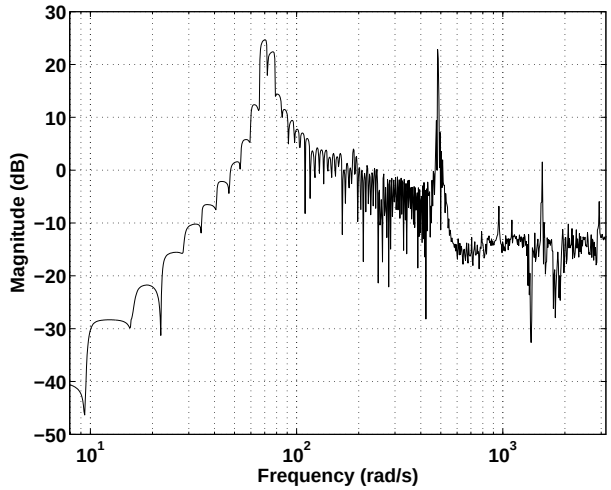

Figure 4. Bode magnitude plot of the transfer function from y to w.

C. Simulation Comparisons

Before the control algorithms are put into experiments, simulation comparisons are first done for the following four control algorithms which may be applied to the control of flexible beam system. The parameters of the plant used for the simulation are selected to be the same as actual plant parameters. The four control algorithms and their parameter calculations are listed as follows:

- Proposed control approach (**C1**): The vector of the feedback gain of the inner-loop controller is chosen to be $\mathbf{K} = [38\ 38\ 12000\ 150]$. The term $12000e_{pb} + 150\dot{e}_{pb}$ is the high-gain PD term to regulate the base position as fast and accurate as possible around the desired target. The term $38e_q + 38\dot{e}_q$ is the deflection feedback term with relatively low gain to dampen the vibration of the beam while not magnifying the high-frequency vibration modes. The resulting eigenvalues of $\mathbf{A}-\mathbf{BK}$ are -219.87, -133.13, $-1.2-73.79i$, $-1.2+73.79i$. It is obvious that with the above feedback control law in the inner loop, the exponential converging rate of e_{pb} and $\dot{e}_{pb}$ are much faster than that of e_q and $\dot{e}_q$. Thus, when choosing $\mathbf{Q}$, the weights on the 3rd and 4th coordinates need to be much larger than the 1st and 2nd coordinates to avoid getting an ill-shaped $\mathbf{P}$. We choose $\mathbf{Q} = diag\{\varphi_1(L)^2, 0.01\varphi_1(L)^2, 10^{11}, 10^6\}$. $\mathbf{P}$ can then be obtained by solving the Lyapunov equation with the above $\mathbf{Q}$. $\varepsilon = 1.653$, $c_2 = 0.5$, $c_1 = 0.4$. With the above choices of parameters, $\mathbf{PB} = 10^6 \times [-0.0526\varphi_1(L),\ 0.00001,\ 4.1667,\ 0.0155]^T$, which means that the term $\hat{\Delta}$ is almost the same as the traditional integrator term for the control of the base position. The integration gain γ is taken as $10000/(4.1667 \times 10^6)$. The inner-loop control law is implemented with sampling rate $5kHz$, which is a relatively high sampling rate, and the trajectory generation algorithm is implemented in the outer loop with a much larger sampling period of $T = 0.02sec$.
- Linear state feedback approach (**C2**): A traditional linear state-feedback controller is also designed and implemented for comparison purpose. The linear controller has the form $u = -\mathbf{K}(\mathbf{x}-\mathbf{x_c}) - \gamma\mathbf{B^T P}\int_0^t(\mathbf{x}(\tau)-\mathbf{x_c}(\tau))d\tau$, where $\mathbf{x_c} = [0,0,p_c,0]^T$ and p_c is the reference command. The controller gains $\mathbf{K}$ and γ are chosen to be the same as in **C1**. In other words, the controller to be compared with is a pure linear version of the proposed inner-loop control law without outer-loop trajectory replanning algorithm.
- PID control for the linear motor only without considering the flexibility of the beam (**C3**): To see the importance of dampening the beam deflection, a traditional PID control law for the linear motor stage only without beam deflection feedback is also used for comparison. The PID control law is $u = M\ddot{p}_{br}(t) - k_p(p_b - p_{br}(t)) - k_i\int_0^t(p_b(\tau) - p_{br}(\tau))d\tau - k_d(\dot{p}_b(t) - \dot{p}_{br}(t))$. The controller gains are selected to be same as those in **C1** and **C2**, i.e., $k_p = 12000$, $k_d = 150$ and $k_i = 10000$. The reference trajectory of the base $p_{br}(t)$ is taken to be an S-curve from 0 to 0.4 with $14m/sec^2$ maximum acceleration and $2m/s$ maximum velocity, which has already been proved to be the time-optimal trajectory for point-to-point movement of a 2nd-order linear motor system with velocity and acceleration constraints [30].
- Asymptotically stable end-point regulation algorithm proposed in [6] (**C4**): The control law is

$u = -k_p(p_b(t) - p_{br}(t)) - k_d(\dot{p}_b(t) - \dot{p}_{br}(t)) - k_g g(t) \cdot \text{sgn}(\dot{p}_b(t)) \int_0^t |\dot{p}_b(\tau)| g(\tau) d\tau$, which consists of a traditional PD feedback term and an addition vibration feedback term. In the simulation, $g(t)$ is taken to be the strain at the base of the beam, just as in [6]. k_p, k_d and the reference trajectory $p_{br}(t)$ are selected to be the same as in **C3**. $k_g = 10000$ is used as the gain of vibration feedback term.

The desired target p_{ed} for the output is set to be a square wave that switches between $0m$ and $0.4m$ every $15sec$. This point-to-point movement is widely used in industry. The reference command for the controller **C2** is set to be a chopped ramp signal between $0m$ and $0.4m$ with a slope of $0.5m/s$.

The tip positions of the systems with four controllers are plotted in Fig 5. It is seen that, all controllers can drive the tip position close to the desired target in a finite time. **C1**, **C3** and **C4** have almost equally fast transient response speed while **C2** has a slower response speed because the use of a slower chopped ramp signal as the reference trajectory to track during the transient. The control inputs and beam deflections during the transient period are plotted in Fig 6 and Fig 7, respectively. From the figures, it is seen that the beam vibrations are very strong for **C2** and **C3**. The constraints on beam deflections (within $\pm 0.005m$) are already violated for these two controllers. Though **C2** uses a slower chopped ramp signal as the reference trajectory, it did not help much to reduce the amplitude of beam vibration during the transient period. **C3** completely ignores the flexibility of the beam and thus the beam vibration is very severe during the transient period and persists for a very long time thereafter. By introducing the base strain feedback, **C4** reduces the vibration of the beam, but the vibration amplitude is still as high as $0.006m$. In comparison, the beam deflection of **C1** is very smooth and has almost no visible vibration due to the use of online trajectory replanning in the overall control scheme.

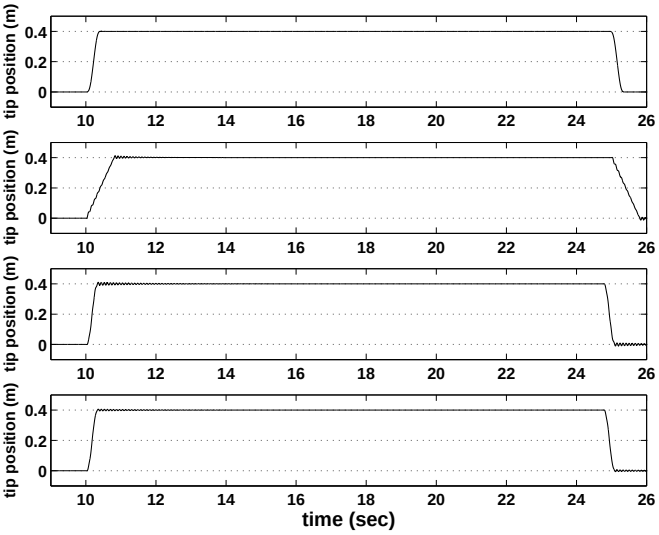

Figure 5. Tip positions for **C1**, **C2**, **C3** and **C4** in simulation.

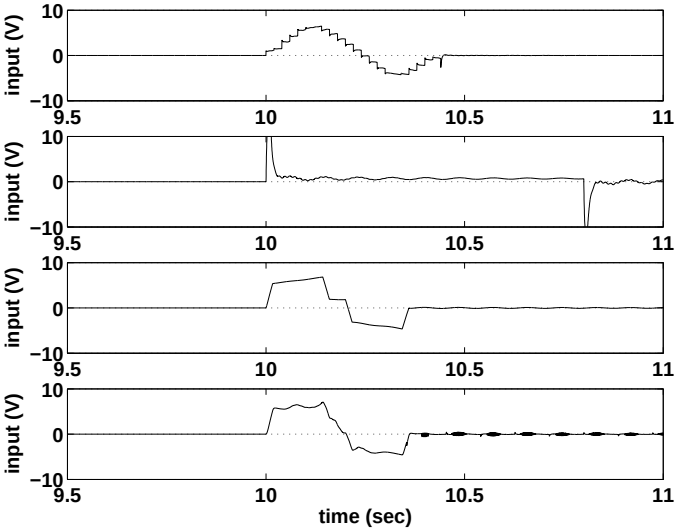

Figure 6. Control inputs during the transient period for **C1**, **C2**, **C3** and **C4** in simulation.

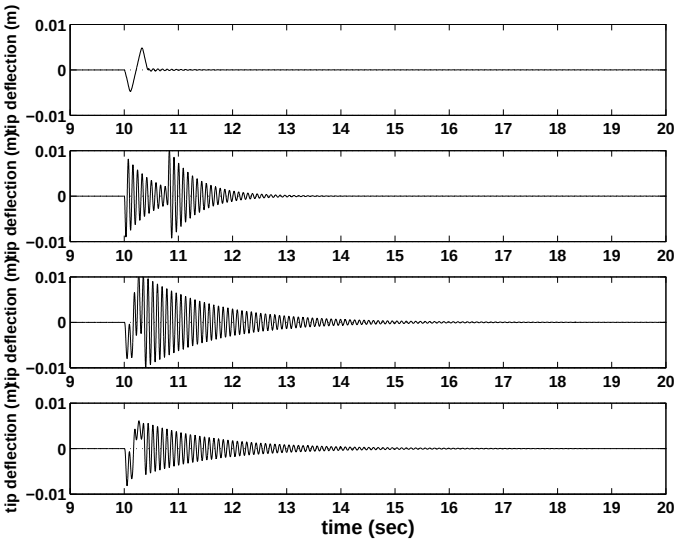

Figure 7. A plot of beam deflections during transient period for **C1**, **C2**, **C3** and **C4** in simulation.

D. Experimental Results

Next, to see the practicality of the proposed controller and its effect to reduce beam vibration in actual implementation, the proposed algorithm (**C1**) and PID control for the linear motor only without considering the flexibility of the beam (**C3**) are experimentally tested and the results are compared. The desired trajectory is the same as that in the simulation case. The plots of tip positions of the systems with two controllers are similar to those in the simulation. The control inputs and the beam deflections during the transient period are plotted in Fig 8 and Fig 9, respectively. It is seen that the experimental results correspond to the simulation results very well. With the proposed algorithm, the vibration of the beam in actual experiment is significantly reduced (almost invisible) compared to the case when a simple PID control

law with no active damping of beam vibration is used. The beam deflections, the velocities of deflections, base positions and base velocities for **C1** during the transient period are also plotted in Fig 10. From the figures, it is seen that all the state constraints are indeed satisfied during the actual experiment, clearly validating the proposed theoretical results on the constraints satisfaction.

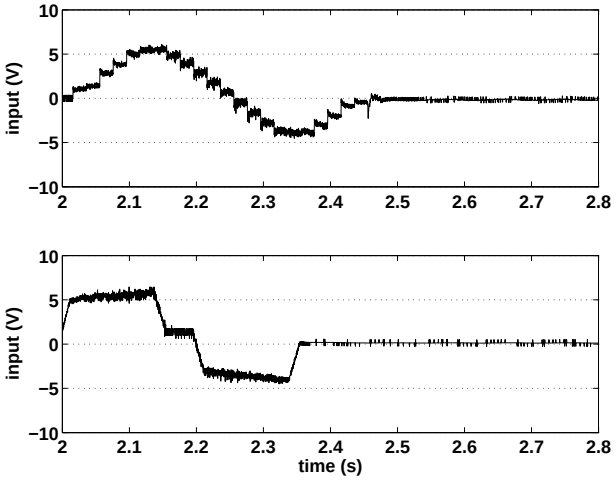

Figure 8. Control inputs during the transient period for **C1** and **C3** in actual experiments.

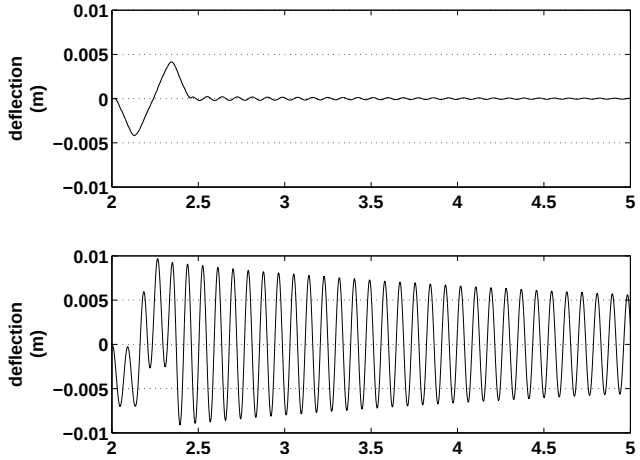

Figure 9. A plot of beam deflections during transient period for **C1** and **C3** in actual experiments.

IX. Conclusion

In this paper, a new approach for the constrained tip tracking control of a linear motor driven flexible beam system is proposed. The proposed control strategy has a hybrid structure with two loops. In the inner loop, a nonlinear feedback control law is designed and implemented in continuous-time domain to keep the tracking error with respect to the replanned trajectory within certain small positive invariant set while achieving good disturbance rejection capability at steady state. In the outer loop, a trajectory regeneration algorithm is implemented

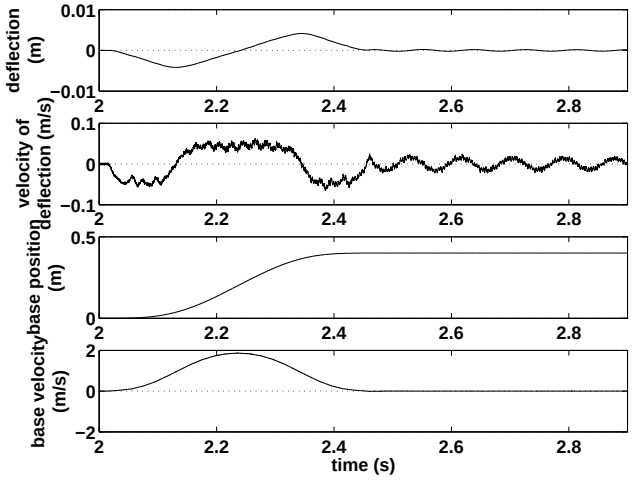

Figure 10. Beam deflections, the velocity of deflections, base positions and base velocities during the transient period for **C1** in actual experiments.

in discrete-time domain to produce a replanned trajectory that converges to the desired target as fast as possible while satisfying all the constraints. With this two-loop approach, fast transient converging rate of the tracking error and good steady-state tracking accuracy can be achieved simultaneously, as shown in the theoretical results. A HIWIN linear motor stage with a flexible beam clamped to the base is then used as the hardware to test practicality of the proposed algorithm in actual implementation. Comparative simulation and experimental results obtained all show that the closed-loop system can indeed achieve the theoretically predicted performances.

References

[1] C. Hu, B. Yao, and Q. Wang. Coordinated adaptive robust contouring controller design for an industrial biaxial precision gantry. *IEEE/ASME Transactions on Mechatronics*, 15(5):728–735, October 2010.

[2] Chuxiong Hu, Bin Yao, and Qingfeng Wang. Coordinated adaptive robust contouring control of an industrial biaxial precision gantry with cogging force compensations. *IEEE Transactions on Industrial Electronics*, 57(5):1746–1754, May 2010.

[3] Chuxiong Hu, Bin Yao, and Qingfeng Wang. Global task coordinate frame based contouring control of linear-motor-driven biaxial systems with accurate parameter estimations. *IEEE Transactions on Industrial Electronics*, 58(11):5195–5205, June 2011.

[4] Bin Yao, C. Hu, and Q. Wang. An orthogonal global task coordinate frame for contouring control of biaxial systems. *IEEE/ASME Transactions on Mechatronics*, 17(4), August 2012. (in press and available on line with DOI 10.1109/TMECH.2011.2111377).

[5] D. Sepasi, R. Nagamune, and F.Sassani. Tracking control of flexible ball screw drives with runout effect and mass variation. *IEEE Transactions on Industrial Electronics*, 59(2):1248–1256, February 2012.

[6] Shuzhi Sam Ge, T. H. Lee, and G. Zhu. Asymptotically stable end-point regulation of a flexible scara/cartesian robot. *IEEE/ASME Transactions on Mechatronics*, 3(2):138–144, 1998.

[7] Shuzhi Sam Ge, Wei He, Bernard Voon Ee How, and Yoo Sang Choo. Boundary control of a coupled nonlinear flexible marine riser. *IEEE Transactions on Control Systems Technology*, 18(5):1080–1091, 2010.

[8] Yoshiyuki Sakawa, Fumitoshi Matsuno, and Shigenobu Fukushima. Modeling and feedback control of a flexible arm. *Journal of Robotic Systems*, 2(4):453–472, 1985.

[9] Bruno Siciliano. A singular perturbation approach to control of lightweight flexible manipulators. *The International Journal of Robotics Research*, 7(4):79–90, 1988.

[10] A. De Luca and B. Siciliano. Trajectory control of a nonlinear one-link flexible arm. *Int. J. Contr.*, 50(5):1699âĂŞ1715, February 1989.

[11] H. Geniele, R. V. Patel, and K. Khorasani. End-point control of a flexible-link manipulator: theory and experiments. *IEEE Transactions on Control Systems Technology*, 5(6):556–569, 1997.

[12] Bo Xie and Bin Yao. Multi-objective optimization of tip tracking control using lmi. In *Proceeding of ASME International Mechanical Engineering Congress and Exposition*, pages 1533–1542, 2005.

[13] S. E. Talole, J. P. Kolhe, and S. B. Phadke. Extended-state-observer-based control of flexible-joint system with experimental validation. *IEEE Transactions on Industrial Electronics*, 57(4):1411–1419, 2010.

[14] E. Polak and T. H. Yang. Moving horizon control of linear systems with input saturation and plant uncertainty. ii: disturbance rejection and tracking. *International Journal of Control*, 58(3):639–663, 1993.

[15] D. Q. Mayne, J. B. Rawlings, C. V. Rao, and P. O. M. Scokaert. Constrained model predictive control: stability and optimality. *Automatica*, 36(6):789–814, 2000.

[16] Francesco Borrelli. *Constrained optimal control of linear and hybrid systems*. Springer, 2003.

[17] U. Maeder, F. Borrelli, and M. Morari. Linear offset free model predictive control. *Automatica*, 45(10):2214–2222, 2009.

[18] Bin Yao, C. Hu, L. Lu, and Q. Wang. Adaptive robust precision motion control of a high-speed industrial gantry with cogging force compensations. *IEEE Transaction on Control System Technology*, 19(5):1149–1159, September 2011.

[19] L. Lu and Bin Yao. Globally stable fast tracking control of a chain of integrators with input saturation and disturbances: a holistic approach. In *Proceedings of American Control Conference*, pages 4434–4439, San Francisco, CA, 2011. (the revised full version is submitted to *ASME Journal of Dynamic Systems, Measurement and Control*).

[20] Y. F. Li and X. B. Chen. End-point sensing and state observation of a flexible-link robot. *IEEE/ASME Transactions on Mechatronics*, 6(3):351–356, 2001.

[21] Bin Yao. Integrated direct/indirect adaptive robust control of SISO nonlinear systems transformable to semi-strict feedback forms. In *American Control Conference*, pages 3020–3025, 2003. The O. Hugo Schuck Best Paper (Theory) Award from the American Automatic Control Council in 2004.

[22] C. Hu, B. Yao, and Q. Wang. Integrated direct/indirect adaptive robust contouring control of a biaxial gantry with accurate parameter estimations. *Automatica*, 46(4):701–707, April 2010.

[23] Chuxiong Hu, Bin Yao, and Qingfeng Wang. Adaptive robust precision motion control of systems with unknown input dead-zones: a case study with comparative experiments. *IEEE Transactions on Industrial Electronics*, 58(6):2454–2464, June 2011.

[24] Lu Lu, Zheng Chen, Bin Yao, and Qingfeng Wang. Desired compensation adaptive robust control of a linear-motor-driven precision industrial gantry with improved cogging force compensation. *IEEE/ASME Transactions on Mechatronics*, 13(6):617–624, 2008.

[25] Lu Lu, Bin Yao, Qingfeng Wang, and Zheng Chen. Adaptive robust control of linear motors with dynamic friction compensation using modified lugre model. *Automatica*, 45(12):2890–2896, 2009.

[26] J. Bontsema and Ruth F. Curtain. A note on spillover and robustness for flexible systems. *IEEE Transactions on Automatic Control*, 33(6):567–569, 1988.

[27] M. Kvasnica, P. Grieder, and M. Baotic. *Multi-Parametric Toolbox (MPT), available at http://control.ee.ethz.ch/mpt/*. 2004.

[28] E. Kerrigan. *Matlab Invariant Set Toolbox, available at http://www-control.eng.cam.ac.uk/eck21/matlab/invsetbox/index.html*. 2005.

[29] C. Hu, Bin Yao, and Q. Wang. Performance oriented adaptive robust control of a class of nonlinear systems preceded by unknown dead-zone with comparative experimental results. *IEEE/ASME Transactions on Mechatronics*, 2013. (in press and available on line with DOI 10.1109/TMECH.2011.2162633).

[30] Keun-Ho Rew and Kyung-Soo Kim. A closed-form solution to asymmetric motion profile allowing acceleration manipulation. *IEEE Transactions on industrial electronics*, 57(7):2499–2506, July 2010.

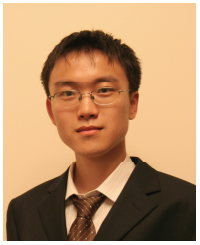

Lu Lu received his B.Eng degree in Mechatronic Control Engineering from Zhejiang University in China in 2008. He is currently a direct PhD student in the School of Mechanical Engineering at Purdue University.

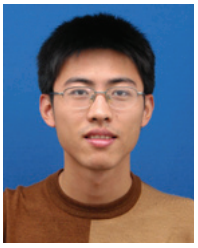

Zheng Chen is currently a direct PhD student in Mechatronic Control Engineering at Zhejiang University in China, from which he received his B.Eng degree in 2007. He was a visiting scholar in the School of Mechanical Engineering at Purdue University from 2008 to 2010.

Bin Yao received his PhD degree in Mechanical Engineering from the University of California at Berkeley in 1996 after obtaining M.Eng. degree in Electrical Engineering from Nanyang Technological University of Singapore in 1992 and B.Eng. in Applied Mechanics from Beijing University of Aeronautics and Astronautics of China in 1987. He has been with the School of Mechanical Engineering at Purdue University since 1996 and was promoted to the rank of Professor in 2007. He was honored as a Kuang-piu Professor in 2005 and a Changjiang Chair Professor at Zhejiang University by the Ministry of Education of China in 2010 as well.

Dr. Yao is the recipient of a NSF CAREER Award in 1998, a NSFC Joint Research Fund for Outstanding Overseas Chinese Young Scholars in 2005, the O. Hugo Schuck Best Paper (Theory) Award from the American Automatic Control Council in 2004, and the Outstanding Young Investigator Award of ASME Dynamic Systems and Control Division (DSCD) in 2007. He has chaired numerous sessions and served in a number of International Program Committee of various IEEE, ASME, and IFAC conferences including the General Chair of the 2010 IEEE/ASME International Conference on Advanced Intelligent Mechatronics. He was a Technical Editor of the IEEE/ASME Transactions on Mechatronics and an Associate Editor of the ASME Journal of Dynamic Systems, Measurement, and Control. More detailed information can be found at `https://engineering.purdue.edu/~byao`

Qingfeng Wang received his Ph.D. and M.Eng. degrees in Mechanical Engineering from Zhejiang University, China, in 1994 and 1988 respectively. He then became a faculty at the same institution where he was promoted to the rank of Professor in 1999. He was the Director of the State Key Laboratory of Fluid Power Transmission and Control at Zhejiang University from 2001 to 2005 and currently serves as the Head of the Institute of Mechatronic Control Engineering. His research interests include the electro-hydraulic control components and systems, hybrid power system and energy saving technique for construction machinery, and system synthesis for mechatronic equipment.